DETERMINATION OF SATURATION FUNCTIONS OF TIGHT CORE SAMPLES BASED ON MEASURED SATURATION PROFILES

C. M. Nielsen, Technical University of Denmark; J. K. Larsen, Technical University of Denmark; N. Bech, Geological Survey of Denmark and Greenland; J. Reffstrup, Dansk Olie & Naturgas A/S; D. Olsen Geological Survey of Denmark and Greenland.

ABSTRACT

The end effect of displacement experiments on low permeable porous media is used for determination of relative permeability functions and capillary pressure functions. Saturation functions for a drainage process are determined from a primary drainage experiment. A reversal of the flooding direction creates an intrinsic imbibition process in the sample, which enables determination of imbibition saturation functions. The saturation functions are determined by a parameter estimation technique. Scanning effects are modelled by the method of Killough. Saturation profiles are determined by NMR.

INTRODUCTION

Laboratory determinations of saturation functions in low permeable structures are complicated by strong scale effects, particularly by the end effect. This capillary retention of the wetting phase in displacement experiments results in a saturation gradient through the core. Although being a problem in many traditional core analyses the end effect actually contains detailed information about the saturation functions of the structure, and can cover a large saturation interval. The objective of the present work is to make use of this information to calculate relative permeability functions and capillary pressure curves.

The method of Nørgaard *et al*. (1995), which uses the end effect for numerical simulation of capillary pressure functions for a primary drainage process, is improved to allow calculation of both drainage and imbibition saturation functions.

A 1D NMR imaging technique is used for quantification of the end effect (Olsen *et al*., 1996). However, the presented method is not dependent on a specific technique for quantifying the end effect. Gamma ray attenuation, CT scanning (Chardaire-Rivière *et al*., 1992) or microwave scanning techniques (Honarpour *et al*., 1995) may be suitable.

THEORY

In a core sample the relation between a gradient in pressure and the flow rate is described by the law of Darcy. Assuming the flow to be one dimensional and horizontal this relation is written for the two fluid phases

$$\frac{dp_o}{dx} = -\frac{m_o}{kk_{ro}}\frac{q_o}{A} \quad (1)$$

$$\frac{dp_w}{dx} = -\frac{m_w}{kk_{rw}}\frac{q_w}{A} \quad (2)$$

In a situation where oil is the non-wetting phase and water is the wetting phase, the capillary pressure is given by

$$p_c = p_o - p_w \quad (3)$$

Given enough time, flooding the sample at constant rate results in an equilibrium situation, where only the displacing fluid is flowing. Eqs. (1-2) show that the pressure gradient in the displaced phase is zero and the phase pressure of this fluid is uniform throughout the sample. Then the capillary pressure can be calculated from Eq. (3) by determining the phase pressure of the displacing fluid along the sample. If the saturation is known as a function of position, the capillary pressure curve can be obtained for the saturation interval defined by the end effect. In the present study the saturation profile of the sample and the phase pressures at the inlet and outlet are measured. The pressure profiles are calculated by integration of the Darcy equations, Eqs. (1) and (2). To perform the integration, the relative permeabilities as functions of saturation must be determined. This is done by use of transient and steady state data from the displacement experiments, by a parameter estimation technique, described below. The description of the procedure is divided into a drainage and an imbibition part.

Drainage

The procedure will determine the relative permeabilities and the capillary pressure for a primary drainage process. The gradient in capillary pressure at steady state ($dp_w/dx = 0$) may be written, by use of Eqs. (1-3)

$$\frac{dp_c}{dx} = -\frac{m_o}{kk_{ro}}\frac{q_o}{A} \quad (4)$$

Assuming p_c to be a function of saturation, $f_c(S_w)$,the gradient in water saturation is given by

$$\frac{dS_w}{dx} = -\frac{m_o}{kk_{ro}}\frac{q_o}{A}\frac{1}{\frac{df_c}{dS_w}} \quad (5)$$

Eqs. (4) and (5) can be solved with the boundary conditions

$$p_c(x=0) = p_{in} - p_{out} \quad (6)$$

$$p_c(x=L) = 0 \quad (7)$$

$$S_w(x=0) = S_{wi} \quad (8)$$

and the relationships

$$k_{ro}(S_w) = f_o(a_1, a_2, ..., a_l, S_w) \quad (9)$$

$$p_c(S_w) = f_c(b_1, b_2, ..., b_l, S_w) \quad (10)$$

The saturation functions are represented by functional relationships of the water saturation. The relative permeability to oil and the capillary pressure are determined by using the measured saturation profile together with the total pressure drop over the sample, (p_{in}-p_{out}).
For a given set of coefficients a_i and b_i in Eqs. (9) and (10) the capillary pressure, p_c, and the water saturation, S_w, are calculated from Eqs. (4) and (5) and the boundary conditions in Eqs. (6-8). The coefficients, a_i and b_i are determined so that they minimise the following least square objective function, by use of a standard non-linear least square solver

$$J_o(\vec{a}, \vec{b}) = \sum_{i=1}^{M} \left(S_w^c(x_i) - S_w^m(x_i) \right)^2 + \left(\Delta p_T^c - \Delta p_T^m \right)^2 + \left(p_{th}^c - p_{th}^m \right)^2 \quad (11)$$

The objective function is a sum of squared residuals, which are the differences in the calculated and measured values for the water saturation along the sample, the difference in total pressure and the difference in the capillary threshold pressure. The squared residuals are weighted to make their contribution to the objective function similar in size. By Eqs. (4-11) the relative permeability to oil and the capillary pressure are determined by iteration.

In order to determine the relative permeability to water the transient part of the drainage experiment is used. The relative water permeability is again represented by a functional relationship of the water saturation

$$k_{rw}(S_w) = f_w(c_1, c_2, ..., c_l, S_w) \quad (12)$$

The coefficients c_i are determined so that they minimise the following least square objective function, by use of the same non-linear least square solver as above

$$J_w(\vec{c}) = \sum_{i=1}^{N} \left(\Delta p_T^c(t_i) - \Delta p_T^m(t_i) \right)^2 \quad (13)$$

The squared residuals are the total pressure difference as function of time during the transient part of the drainage. For a given set of coefficients, c_i , the relative permeability to water is calculated. The relative permeability to oil and the capillary pressure are known from above. These three parameters are then given as input to a reservoir simulator (ECLIPSE 100, 1994), which is used to compute the total pressure drop across the sample during the drainage process.

Imbibition

In order to determine the imbibition part of the saturation functions the end effect is shifted from one end of the core to the opposite by reversing the direction of the oil flow. The development of an end effect at the new outlet follows an intrinsic imbibition process, while the old end effect is broken down by an intrinsic drainage process. The saturation profile at the new outlet can be used in the calculation of the saturation functions for the imbibition

process. Recall that the bounding saturation curves are obtained under the initial condition of S_w = 100% and $S_w = S_{wi}$ for the drainage and imbibition process respectively. The reversed drainage process violates this condition and scanning curves between the bounding saturation functions will therefore control the process. The scanning process is described by a method developed by Killough (1976). The scanning curves are dependent on the local saturation history of the sample.

Only the scanning of the capillary pressure curves is described here. The scanning of the relative permeability functions is described by similar equations. The scanning capillary pressure curves originating from the primary drainage capillary pressure curve are generated by the expressions below. Similar expressions are used for the scanning from the bounding imbibition curve and for the intermediate case of reversal on a scanning curve.

$$p_c = p_{cd} + F\left(p_{ci} - p_{cd}\right) \tag{14}$$

p_{cd} and p_{ci} are the bounding capillary curves for the drainage and imbibition. The local saturation history is accounted for by the factor F (Aziz and Settari, 1979)

$$F = \frac{1}{S_w - S_{why} + e} - \frac{1}{e} \Bigg/ \frac{1}{(1 - S^*_{or}) - S_{why} + e} - \frac{1}{e} \tag{15}$$

Fig. 1 shows the concept of scanning. S_{why} is the point of reversal on the bounding curve, S^*_{or} is the trapped oil saturation and e is a shape factor. S^*_{or} is equal to S_{or} when S_{why}=S_{wi} (bounding curve for imbibition). The trapped oil saturation is calculated as (Land, 1968)

$$S^*_{or} = (1 - S_{why}) \Bigg/ 1 + \left(\frac{1}{S_{or}} - \frac{1}{(1 - S_{wi})} \right)(1 - S_{why}) \tag{16}$$

Calculation of p_c is performed in a way similar to the drainage case, recalling that k_{ro} refers to the imbibition process. For every measured saturation along the sample the F factor can be calculated assuming a value for e. Given p_c from the reversed imbibition profile and p_{cd} from the drainage, then p_{ci} can be determined from Eq. (14).

EXPERIMENTAL

NMR fluid saturation profile determination

The flow regime considered is essentially one dimensional, along the length of a core sample, when care is taken to align the length of the sample parallel to any layering or lamination present. A one dimensional fluid saturation determination method is therefore appropriate, and an NMR technique was developed for the purpose (Olsen *et al.*, 1996, Olsen, 1997). The technique is based on an NMR pulse sequence that is remarkably simple, consisting of a spin echo sequence with phase-encoding, but without slice selection or read-out gradients. Signals are acquired as asymmetric echoes in order to keep echo time (TE) as short as possible. The cost of acquiring an asymmetric echo instead of a symmetric echo is a decrease in frequency resolution, which in the present case is subordinate to the improvement in minimum echo time, TE_{min}. At present, the shortest possible TE_{min} is

2.4 ms. The pulse sequence is unaffected by chemical shift artifacts in the spatial dimension, and is tolerant to flow. By using a non-magnetic core holder and a Mobile Flooding Unit, described elsewhere (Nørgaard *et al*., 1995), the NMR technique may be applied while core flooding is in progress.

A 4.7 T SISCO scanner was used for the NMR measurements. 1D fluid saturation profiles were obtained with a pixel accuracy better than 5 %-points, and a pixel reproducibility better than 2 %-points ($1\,s$). Spatial resolution is 0.4 mm for a 100 mm profile.

Material and Fluid Data

The material used in the experimental work was chalk of Maastrichtian age from the Danish sector of the North Sea. Results are presented for a 1.5'' plug sample labelled M113. It was cleaned by Soxhlet extraction with methanol and toluene. The porosity and absolute permeability were 26.36% and 0.70 mD respectively. The chalk was water wet and a synthetic formation brine with a salinity of 7%, density of 1048 g/l and viscosity of 1.12 cp at 20°C was used. The non-wetting phase was n-decane with a density and viscosity of 730 g/l and 0.92 cp at 20°C.

Flooding Procedure

To establish both the drainage and imbibition part of the saturation functions a complex flooding procedure is used. The 100% brine saturated sample is first flooded with oil until steady state, production and displacement pressure being recorded. At equilibrium the saturation profile is measured. This stage is represented by the primary oilflood in Fig. 2. The decrease in the brine saturation towards the inlet of the core has been created by a primary drainage process. The oil flow direction is then reversed and the water contained in the end effect is displaced through the sample towards the new outlet, where a new end effect will evolve due to the capillary retention of the water. This build up of an end effect has followed an intrinsic imbibition process. It is done in two steps. First the oil rate is kept at the same rate as the primary drainage. At this condition the new end effect is not fully developed at steady state, Fig. 2. The second step is to increase the flow rate until the pressure gradient matches the pressure gradient at steady state in the primary drainage. The end effect now becomes developed and S_w at the new inlet is forced to the value of S_{wi} obtained at the primary drainage, Fig. 2. The new end effect is used to calculate the spontaneous imbibition part of the saturation functions. The forced imbibition part is obtained by flooding the core with brine in the same direction as the reversed oil flow, resulting in an almost constant saturation through the sample, Fig. 2.

RESULTS AND DISCUSSION

The parameter estimation technique was tested on a model labelled M15A. A set of synthetic saturation functions was used as input to a simulated drainage experiment using a reservoir simulator (ECLIPSE 100, 1994). The resulting saturation profile and production data were then used to determine the saturation functions. The results are shown in Fig. 3 and 4. Good agreement between the calculated results and the input data is found. This

demonstrates that the procedure for calculating drainage saturation functions from a saturation profile and production data is valid for ideal synthetic data.

Experimental data was obtained from a series of flooding experiments performed on the sample M113. The production and pressure data were recorded and at steady state the fluid distribution was measured as shown in Fig. 2. For the drainage case the saturation profile together with the measured total pressure difference were used to determine the relative oil permeability and the capillary pressure curve for the primary drainage, Fig. 5 and 6. Drainage relative permeability data for chalk, that are comparable to Fig. 5, are unknown to the authors. The lack of data is probably due to the fact that it is difficult to generate meaningful results for material with pronounced end effects by means of the standard methods. The verification of the synthetic data set M15A, demonstrates that the calculation procedure can reproduce realistic relative permeability functions. The determined capillary pressure was compared with results obtained from a standard mercury injection technique also presented in Fig. 6. The mercury injection curve was scaled by Leverett's J-function using a standard value of 480 mN/m for the interfacial tension for the mercury-air system and a measured value of 38 mN/m for the oil-water system. No correction for contact angle was applied as the sample was strongly water wet (Anderson, 1987). The shapes of the curves are similar, but the mercury injection data has a wider and more flat plateau. A situation similar to Fig. 6. has been reported previously (Nørgaard *et al*., 1995). In general data from the air-mecury and brine-oil systems cannot be considered directly comparable (Christoffersen, 1992). The threshold pressure for the sample was measured independently by an injection experiment and incorporated into the objective function Eq. (11) for precise location of the plateau of the calculated capillary pressure curve.

The measured steady state saturation profiles from the complex flooding procedure show how the old end effect is displaced through the sample by reversing the flow direction, Fig. 2. From Fig. 1 and 2 follows that the imbibition is controlled by scanning curves starting from the primary drainage curve when the saturation of reversal S_{why} is above S_{wi} . In fact only the first pixel in the new outlet will follow the bounding imbibition curve during the increase in saturation. The scanning curves provide the information to calculate the imbibition bounding curve by use of the scanning method of Killough (1976) as outlined in the theory. The saturation profile from the reversed oilflood with the fully developed end effect will give part of the spontaneous imbibition curve. Information for the forced imbibition curve ($p_c < 0$) is contained in the profile from the reversed waterflood. Fig. 2 shows that the reversed waterflood gives a narrow saturation interval indicating that the sample is strongly water wet. The parameter estimation technique remains to be demonstrated for the imbibition process.

The reversed flooding of M113 produced a hump on the saturation profile, Fig. 2. The hump has a negative saturation gradient on the side towards the outlet of the sample. The hump was examined by the test model M15A. A reversed oilflood was simulated with and without the use of scanning curves, Fig. 7. The simulations without the scanning option failed to produce the hump. The simulations also revealed that the hump is a result of a

complex scanning process, where part of the sample follows more than one scanning curve. This is a consequence of the scanning being a function of the local saturation history. When shifting the end effect obtained from the primary drainage, part of the sample will experience a transient higher water saturation than the final steady state saturation.

CONCLUSIONS

A procedure to determine saturation functions for low permeable structures by a parameter estimation technique has been developed. The procedure utilises the strong capillary retention of the wetting phase in such structures.

* The drainage saturation functions are calculated from a measured saturation profile, the total pressure drop and the threshold pressure from a primary drainage process. The technique was verified on a synthetic test case and good agreement was found between the calculated and the true solution. The calculated capillary pressure curve for a chalk sample was compared with scaled mercury injection data obtained from the same sample. The plateau of the mercury data is situated at a significantly lower capillary pressure.

* A complex flooding procedure is outlined by which the imbibition part of the saturation functions can be calculated. The flooding procedure shifts the end effect to create a saturation profile, where the increase in saturation has followed a spontaneous imbibition process. An additional flooding creates a profile, which has followed a forced imbibition process.

* In order to obtain the imbibition bounding curves for the saturation functions the local saturation history must be described by the use of scanning curves.

* The saturation functions can be obtained from standard flooding experiments with moderate pressure gradients across the sample.

* The technique can be used on native samples and with reservoir like fluids.

Acknowledgement

The Danish Ministry of Environment and Energy is acknowledged for funding the work through the EFP-96 programme. The Danish Research Centre of Magnetic Resonance is acknowledged for providing NMR facilities.

NOMENCLATURE

a	coefficient
$\vec{a}$	parameter vector
A	flow area
b	coefficient
$\vec{b}$	parameter vector
c	coefficient
$\vec{c}$	parameter vector
f	arbitrary function
F	F factor (scanning)
J	objective function
k	absolute permeability
k_r	relative permeability
k_{ro}	relative oil permeability
k_{rw}	relative water permeability
L	length of core sample
M	number of measured saturation points along the sample
N	number of time steps
p	pressure
q	flow rate
S	saturation
t	time
x	direction of flow downstream
e	scanning parametre
m	viscosity

Subscripts

c	capillary pressure
cd	capillary pressure (drainage)
ci	capillary pressure (imbibition)
i	coefficient no. i
in	inlet of core sample
l	number of coefficients
o	oil
or	residual oil saturation
out	outlet of core sample
T	total
th	threshold pressure
w	water
why	point of reversal (scanning)
wi	irreducible water saturation

Superscripts

c	calculated
m	measured
*	trapped oil

REFERENCES

Anderson, W.G., "Wettability Literature Survey - Part 4: Effects of Wettability on Capillary Pressure," *Journal of Petroleum Technology* (Oct. 1987), 1283-1300.

Aziz, K.; Settari, A., *Petroleum Reservoir Simulation*, Elsevier Applied Science Publishers LTD, GB, (1979), 395-401.

Chardaire-Rivière, C.; Chavent, G.; Jaffré, J.; Liu, J.; Bourbiaux, B.J., "Simultaneous Estimation of Relative Permeabilities and Capillary Pressure," *SPE Formation Evaluation*, (Dec. 1992), 283-289.

Christoffersen, K.R., *High-Pressure Experiments with Application to Naturally Fractured Chalk Reservoirs, 1. Constant Volume Diffusion, 2. Gas-Oil Capillary Pressure*, Doctor Dissertation, University of Trondheim, (1992), 214 pages.

ECLIPSE 100 , 95A Release, Intera Information Technologies Ltd., Highlands Farm, Henley-on-Thames, Oxfordshire, U.K. (1994).

Honarpour, M.M.; Huang, D.D.; Dogru, A.H., ”Simultaneous Measurements of Relative Permeability, Capillary Pressure, and Electrical Resistivity with Microwave System for Saturation Monitoring,” *SPE paper 30540*, (1995).

Killough, J.E., “Reservoir Simulation with History-Dependent Saturation Functions,” *SPEJ*, (Feb. 1976).

Land, C.S., “Calculation of Imbibition Relative Permeability for Two- and Three-Phase Flow from Rock Properties,” *SPEJ*, (June 1968) **243**, 149-156.

Nørgaard, J.V.; Olsen, D.; Springer, N.; Reffstrup, J., “Capillary Pressure Curves for Low Permeability Chalk Obtained by NMR Imaging of Core Saturation Profiles,” *SPE paper 30605*, (1995).

Olsen, D., *Quantitative NMR Measurements on Core Samples*, Danmarks og Grønlands Geol. Unders. Rapp. (1997) **35**, 31 pages.

Olsen, D.; Topp, S.; Stensgaard, A.; Nørgaard, J.V.; Reffstrup, J., “Quantitative 1D Saturation Profiles on Chalk by NMR,” *Magnetic Resonance Imaging*, (1996) **14**, No. 7/8, 847-851.

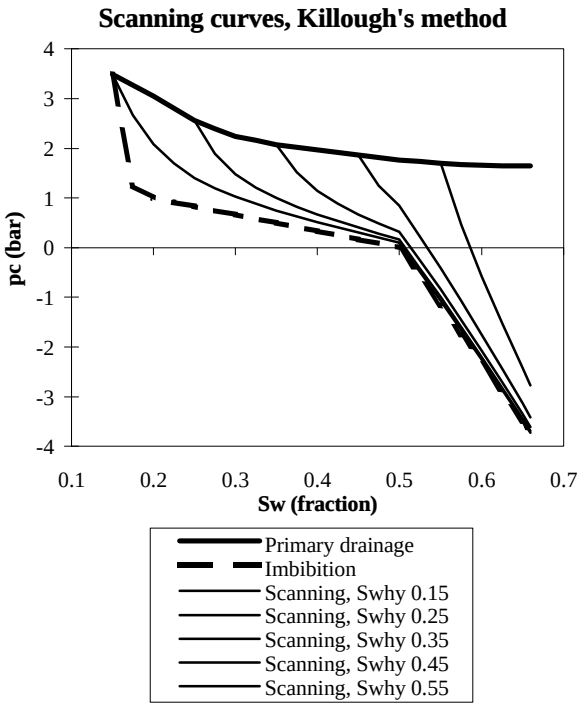

Fig. 1. Example of scanning from the primary drainage capillary pressure.

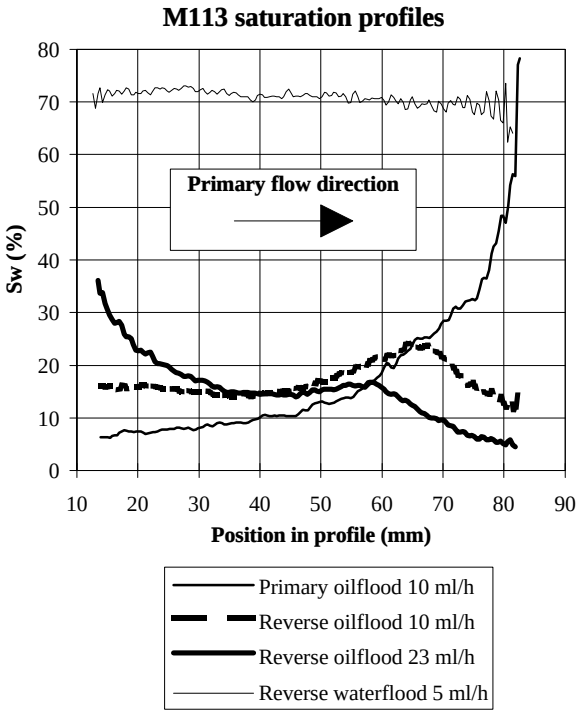

Fig. 2. Measured saturation profiles on sample M113.

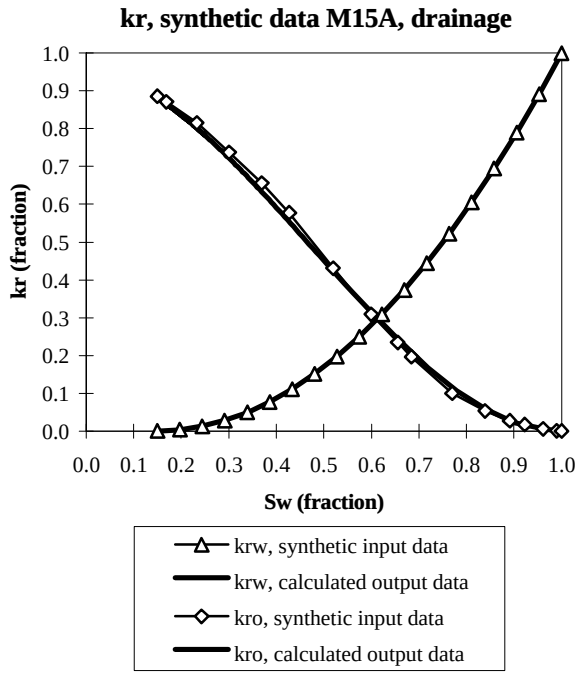

Fig. 3. Verification of synthetic relperm data. k_{ro} is approximated by a polynomial of order three. k_{rw} is approximated by an exponential function.

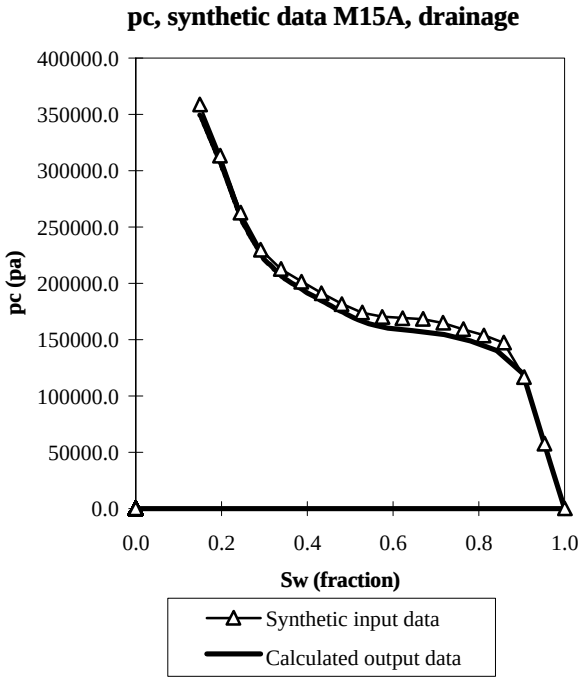

Fig. 4. Verification of synthetic capillary pressure data.

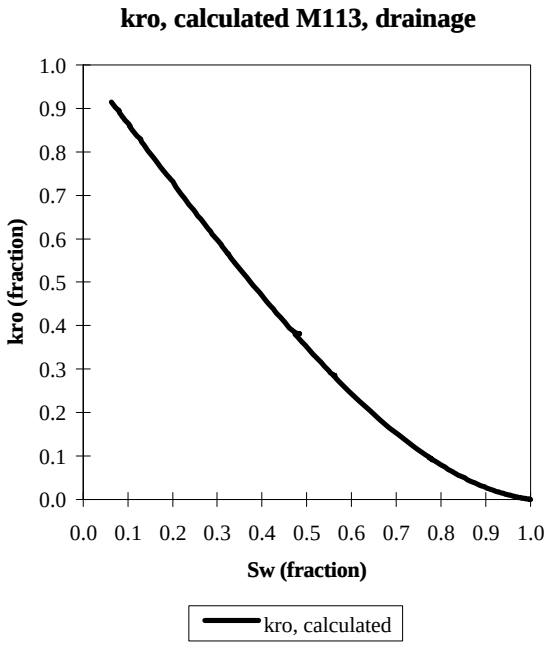

Fig. 5. Measured data. k_{ro} is approximated by a polynomial of order three.

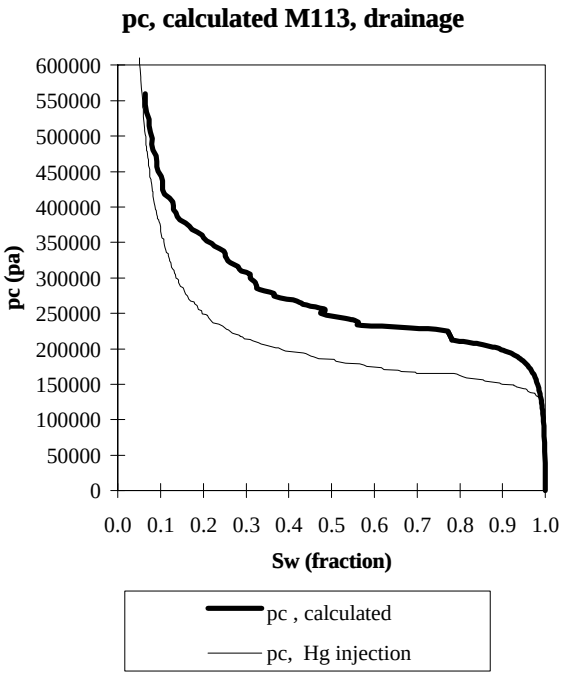

Fig. 6. Measured data. Calculated p_c compared to p_c from Hg injection.

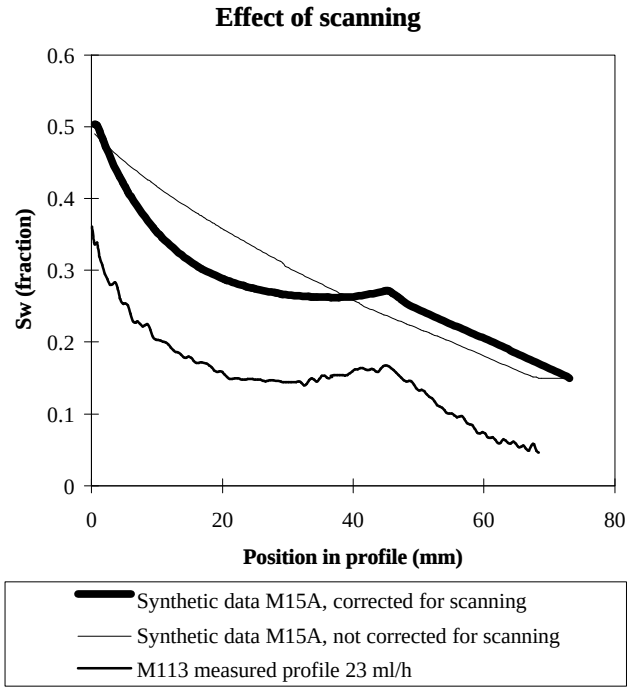

Fig. 7. Qualitative illustration of scanning. The synthetic data M15A were generated with saturation functions differing from sample M113. Therefore the saturation levels differ.